

Supplementary Information

Highly durable carbon-nanofiber-supported Pt–C core–shell cathode catalyst for ultra-low Pt loading proton exchange membrane fuel cells: facile carbon encapsulation

Mohanraju Karuppanan,^{‡a} Youngkwang Kim,^{‡b} Sujin Gok,^a Eunjik Lee,^c Jee Youn Hwang,^c Ji-Hoon Jang,^c Yong-Hun Cho,^d Taeho Lim,^{*e} Yung-Eun Sung^{*bf} and Oh Joong Kwon^{*a}

^aDepartment of Energy and Chemical Engineering, Innovation Center for Chemical Engineering, Incheon National University, 119 Academy-ro, Yeonsu-gu, Incheon 22012, Republic of Korea

^bSchool of Chemical and Biological Engineering, Seoul National University, 1 Gwanak-ro, Seoul 08826, Republic of Korea

^cStrategy & Technology Division, Hyundai motor group, 37 Cheoldobangmulgwan-ro, Uiwang-si 16082, Gyeonggi-do, Republic of Korea

^dDepartment of Chemical Engineering, Kangwon National University, Samchoek, Gangwon-do 25913, Republic of Korea

^eDepartment of Chemical Engineering, Soongsil University, 369 Sangdo-ro, Dongjak-gu, Seoul 06978, Republic of Korea

^fCenter for Nanoparticle Research, Institute for Basic Science (IBS), 1 Gwanak-ro, Seoul 08826, Republic of Korea

[‡]Equally contribute to this work.

^{*}Co-corresponding author

Table S1 Pt loading^a at the MEA cathode^b

	Pt/C	Pt@CS/CNF600	Pt@CS/CNF700	Pt@CS/CNF900
Pt loading	0.102 (± 0.010)	0.104 (± 0.015)	0.104 (± 0.012)	0.101 (± 0.011)

^aUnit: $\text{mg}_{\text{Pt}} \text{cm}^{-2}$

^bThe Pt loading at the MEA anode was measured to be $0.025 \text{ mg}_{\text{Pt}} \text{cm}^{-2}$.

Table S2 Average Pt particle sizes and initial ECSA_{H-upd}s of Pt/C and Pt@CS/CNF

	TEM particle size ^a	XRD crystallite size ^a Pt(111)	ECSA _{H-upd} ^b (half cell)	ECSA _{H-upd} ^b (unit cell)
Pt/C	3.3 (± 0.8)	3.7	69.0 (±1)	50.3 (±10)
Pt@CS/CNF600	3.3 (± 0.7)	4.5	95.6 (±8)	64.1 (±3)
Pt@CS/CNF700	3.6 (± 0.7)	5.6	100.5 (±5)	68.8 (±2)
Pt@CS/CNF900	4.0 (± 0.8)	5.2	99.6 (±9)	73.3 (±4)

^aUnit: nm^bUnit: m² g_{Pt}⁻¹

Table S3 Unit cell performance of the reported ORR catalysts

Catalyst	AST condition	Metal loading ^a	ECSA loss	Voltage loss at 0.8 A cm ⁻²	Ref.
Pt@CS/CNF900	DOE 2016 (30k cycles)	Anode: 0.025 Cathode:0.1	-12%	+1%	In this work
Pt/C@PANI	5k CV cycles (0.6–1.2 V) at a rate of 50 mV s ⁻¹ at 70°C	Anode: 0.3 Cathode: 0.2	–	-80 mV ^a	[1]
PtFe@C	Current sweeping at a rate of 10 mA cm ⁻² s ⁻¹ (OCV–0.35 V) for 100 hr at 80°C	Anode: 0.2 Cathode: 0.2	–	-30 mV ^b	[2]
Pt/CNF	Applying constant potential of 1.4 V at 70°C for 130 hr	Cathode: 0.3	-39% ^a	-160 mV ^b	[3]
Ga-PtNi/C	15k CV cycles (0.6–1.0 V) at a rate of 50 mV s ⁻¹	Anode: 0.15 Cathode: 0.15	–	-30 mV	[4]
AL-PtCo/CN	30k CV cycles (0.6–1.0 V) at a rate of 50 mV s ⁻¹	Anode: 0.1 Cathode: 0.1	-16%	-70 mV ^b	[5]
Pt-Ni cage/C	30k CV cycles (0.6–1.0 V) at a rate of 50 mV s ⁻¹	Anode: N/A Cathode: 0.1	-59%	-60 mV ^b	[6]

^aUnit: mg_{Pt} cm⁻²^bApproximated value

[1] S. Chen, Z. Wei, X. Qi, L. Dong, Y.-G. Guo, L. Wan, Z. Shao and L. Li, *J. Am. Chem. Soc.*, 2012, **134**, 13252–13255.

[2] D. Y. Chung, S. W. Jun, G. Yoon, S. G. Kwon, D. Y. Shin, P. Seo, J. M. Yoo, H. Shin, Y.-H. Chung, H. Kim,

B. S. Mun, K.-S. Lee, N.-S. Lee, S. J. Yoo, D.-H. Lim, K. Kang, Y.-E. Sung and T. Hyeon, *J. Am. Chem. Soc.*, 2015, **137**, 15478–15485.

[3] J. H. Park, S.-M. Hwang, G.-G. Park, S.-H. Park, E.-D. Park and S.-D. Yim, *Electrochim. Acta*, 2018, **260**, 674–683.

[4] J. Lim, H. Shin, M. Kim, H. Lee, K.-S. Lee, Y. Kwon, D. Song, S. Oh, H. Kim and E. Cho, *Nano Lett.*, 2018, **18**, 2450–2458.

[5] W. S. Jung and B. N. Popov, *ACS Sustainable Chem. Eng.*, 2017, **5**, 9809–9817.

[6] X. Peng, S. Zhao, T. J. Omasta, J. M. Roller and W. E. Mustain, *Appl. Catal. B-Environ.*, 2017, **203**, 927–935.

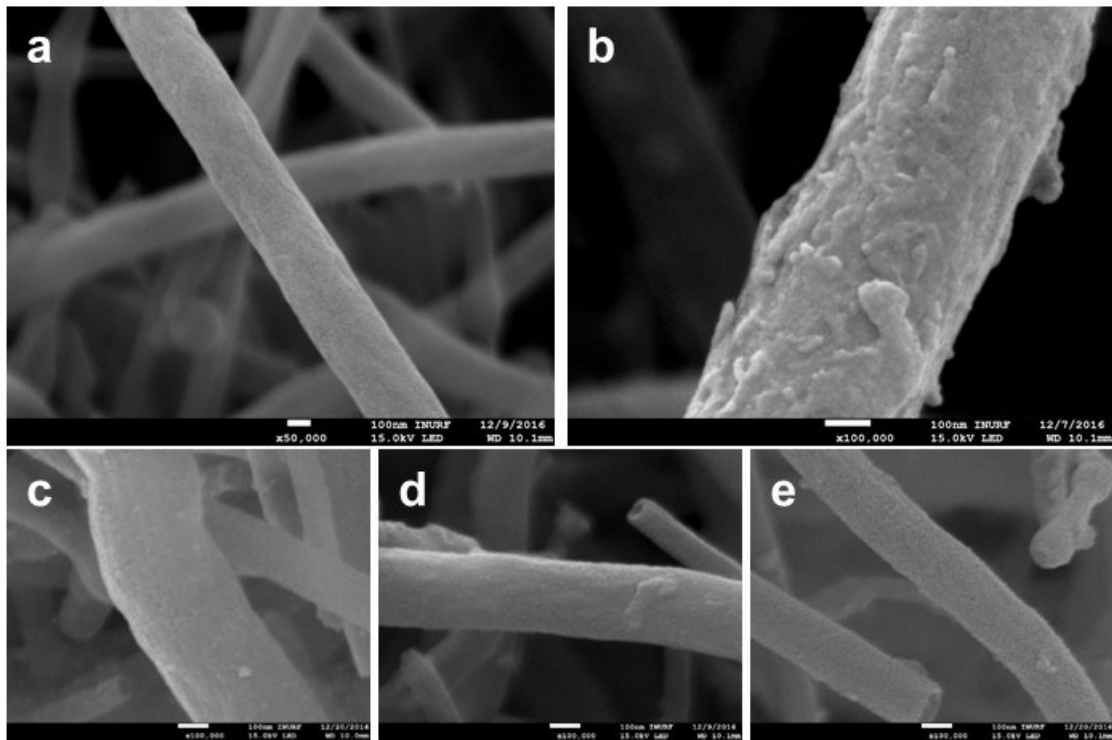


Figure S1 FE-SEM images of (a) bare CNFs, (b) CNFs coated by Pt-aniline complex, (c) Pt@CS/CNF600, (d) Pt@CS/CNF700 and (e) Pt@CS/CNF900.

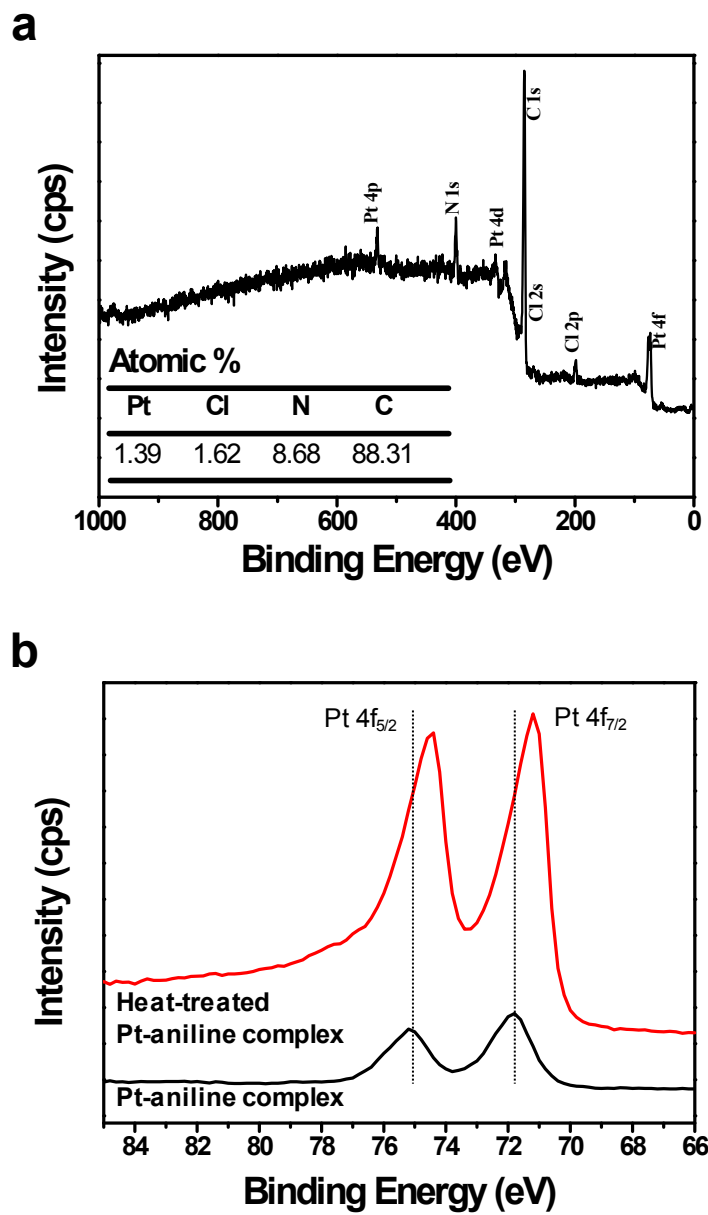


Figure S2 (a) XPS survey spectrum of Pt-aniline complex and (b) Pt 4f spectra of Pt-aniline complex before and after heat treatment. Pt ions in Pt-aniline complex are reduced to metallic Pt by heat treatment.

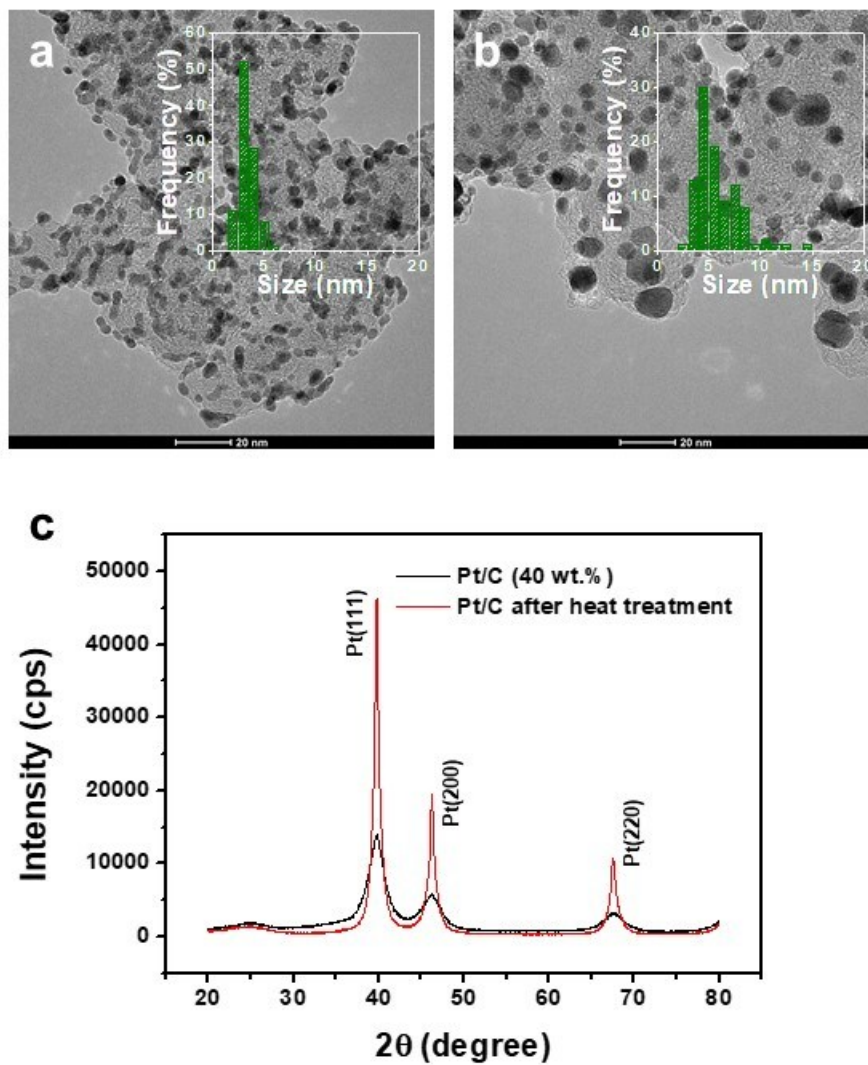


Figure S3 TEM images of Pt/C (20 wt%) (a) before and (b) after the heat treatment at 900°C for 1 hr, and (c) their XRD patterns.

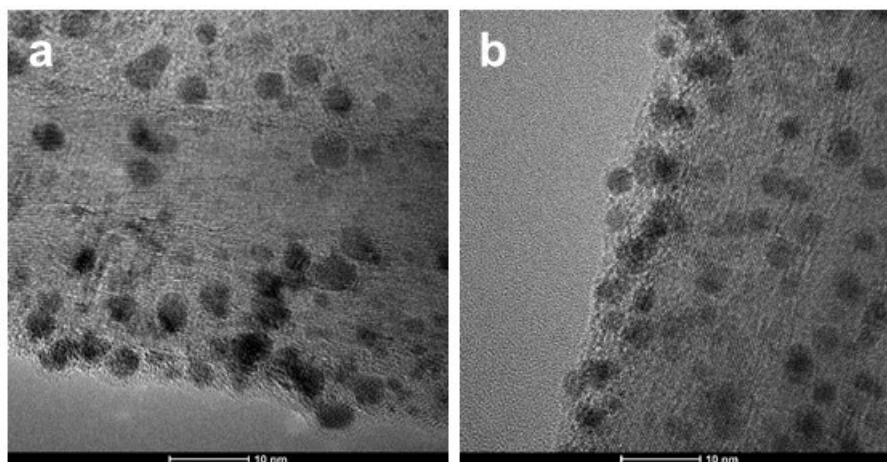


Figure S4 TEM images of (a) CS@Pt/CNF600 and (b) CS@Pt/CNF700.

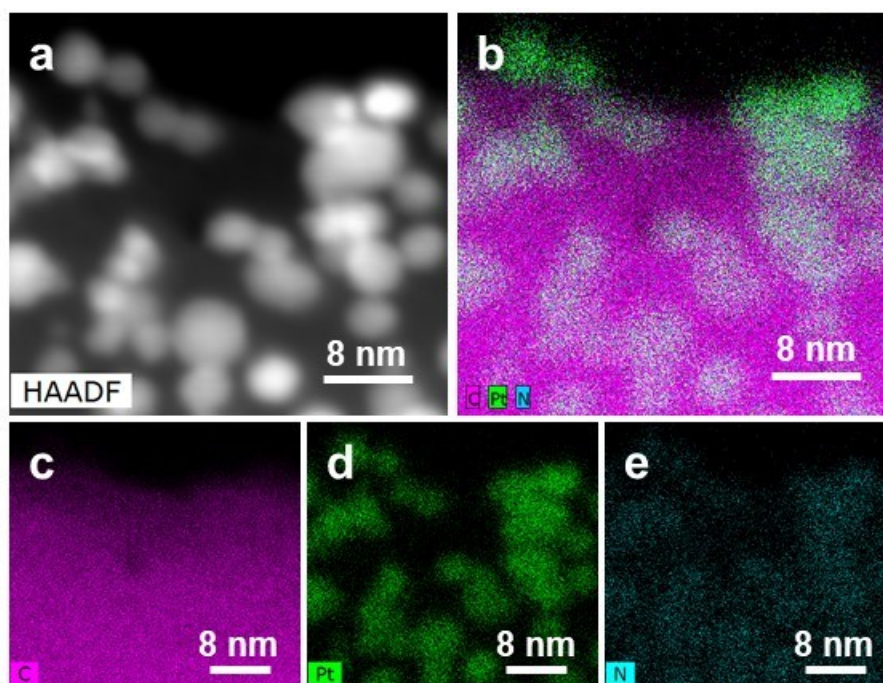


Figure S5 (a) HAADF-STEM image of Pt@CS/CNF900 and (b) superimposition of elemental maps of (c) C, (d) Pt and (e) N.

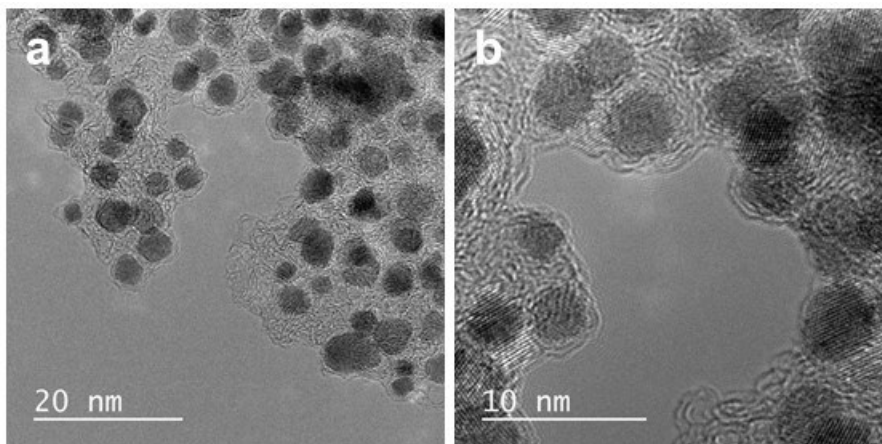


Figure S6 TEM images of Pt-aniline complex (without CNFs) after the heat treatment at 900°C for 1 hr in N₂ atmosphere, (a) low and (b) high magnification.

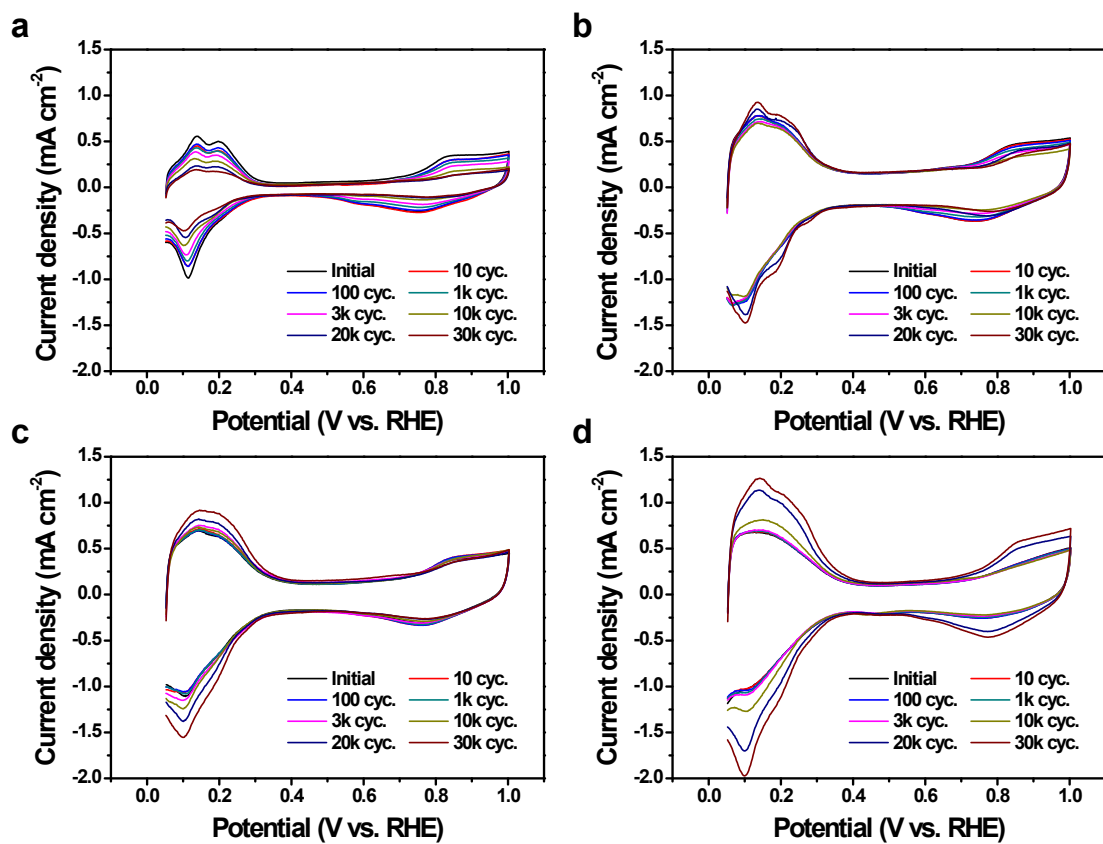


Figure S7 CV curves of (a) commercial Pt/C, (b) Pt@CS/CNF600, (c) Pt@CS/CNF700 and (d) Pt@CS/CNF900 according to the number of AST cycles. The CV curves were obtained in Ar-saturated 0.1 M HClO₄ at a scan rate of 20 mV s⁻¹.

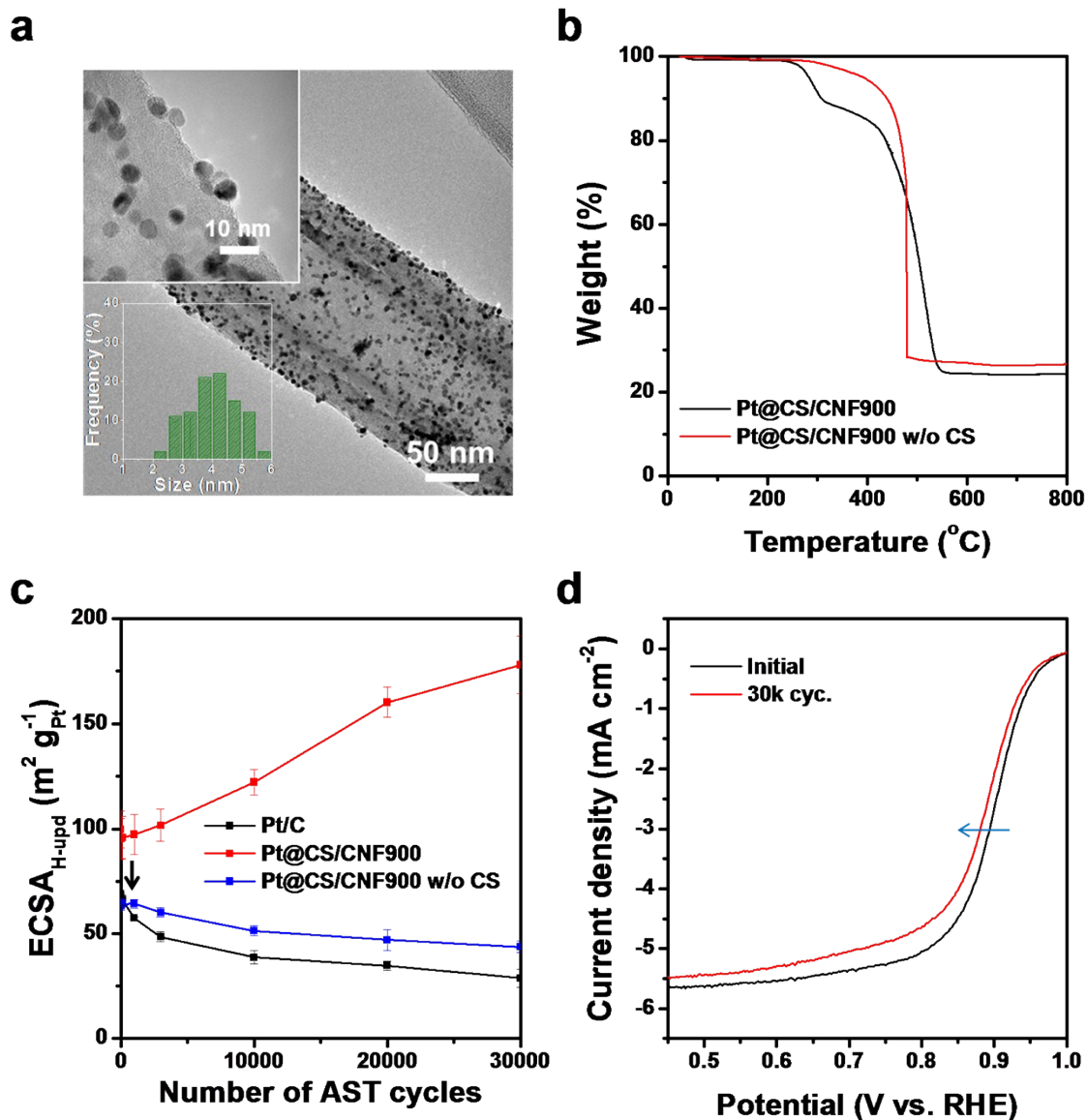


Figure S8 (a) HR-TEM image of Pt@CS/CNF900 after the removal of carbon shells (Pt@CS/CNF900 w/o CS), (b) TGA profiles of Pt@CS/CNF900 before and after the removal of carbon shells, (c) changes in $ECSA_{H-upd}$ of Pt@CS/CNF900 w/o CS according to the number of AST cycles, and (d) ORR polarization curves of Pt@CS/CNF900 w/o CS after the removal of carbon shells. The carbon shell was removed by exposure to air at 300°C for an hour.

After removal of the carbon shell, in Fig. S8a, some agglomerates of Pt nanoparticles were observed because the Pt nanoparticles were no longer protected by the carbon shell. However, the average particle size of the Pt nanoparticles was about 4.1 nm, which was not largely different from that (4.0 nm) before the carbon shell was removed. The removal of the carbon shell was also confirmed by TGA as shown in Fig. S8b: the weight loss stage (225–325°C) associated with the carbon shell, was not observed for Pt@CS/CNF900 w/o CS. As shown in Fig. S8c, it is noteworthy that there was a dramatic decrease in the initial $\text{ECSA}_{\text{H-upd}}$ from 99.6 (± 9) $\text{m}^2 \text{g}^{-1}$ to 64.7 (± 1) $\text{m}^2 \text{g}^{-1}$ after removal of the carbon shells from Pt@CS/CNF900 in spite of the similar average particle sizes of Pt@CS/CNF900 and Pt@CS/CNF900 w/o CS. This is a strong evidence that carbon shells containing N and C atoms contributed the increase in the ECSA. The stability of Pt@CS/CNF900 w/o CS was similar to that of Pt/C due to the absence of the carbon shell (Figs. S8c and d).

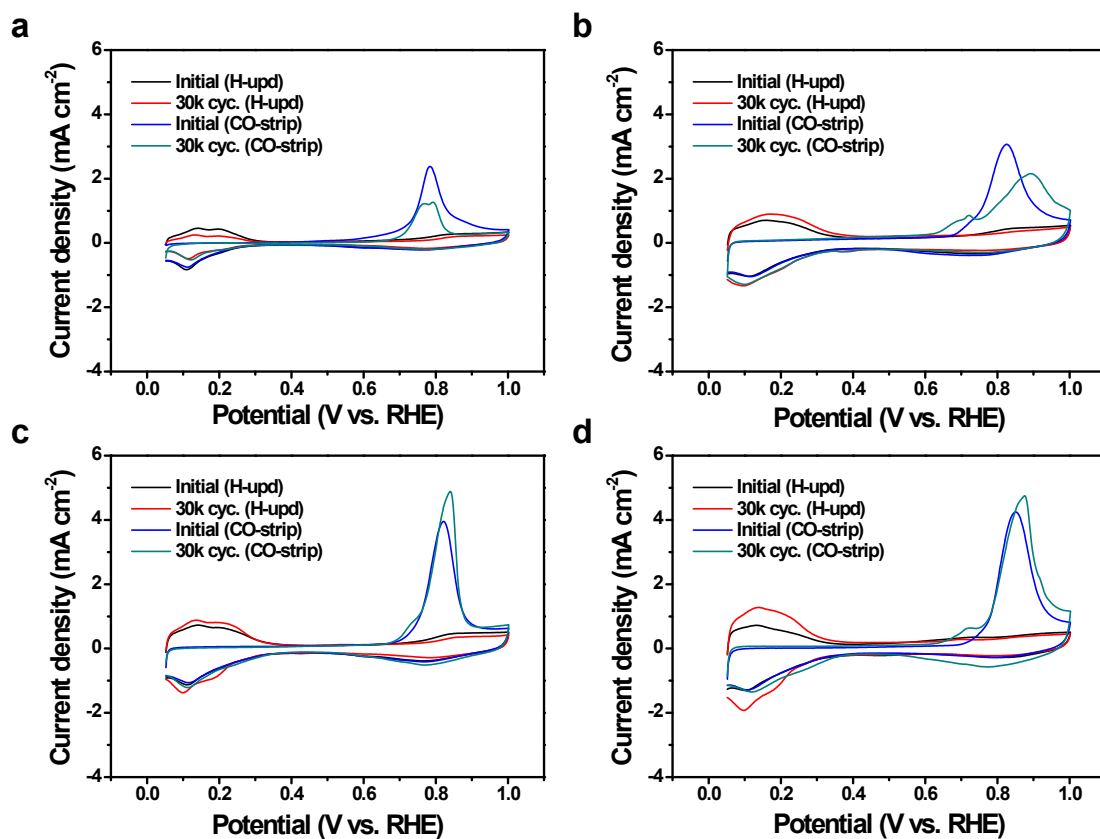


Figure S9 CV curves of (a) commercial Pt/C, (b) Pt@CS/CNF600, (c) Pt@CS/CNF700, and (d) Pt@CS/CNF900 before and after 30k AST cycles. The CV curves were obtained in Ar-saturated 0.1 M HClO₄ at a scan rate of 20 mV s⁻¹. For CO stripping experiment (CO-strip), CO poisoning of Pt was performed at 0.1 V (vs. RHE) with CO (5%) bubbling through the electrolyte for 30 min.¹ After Ar purging for another 30 min, a CV curve was obtained.

[1] T. Binniger, E. Fabbri, R. Kötz and T. J. Schmidt, *J. Electrochem. Soc.*, 2014, **161**, H121–H128.

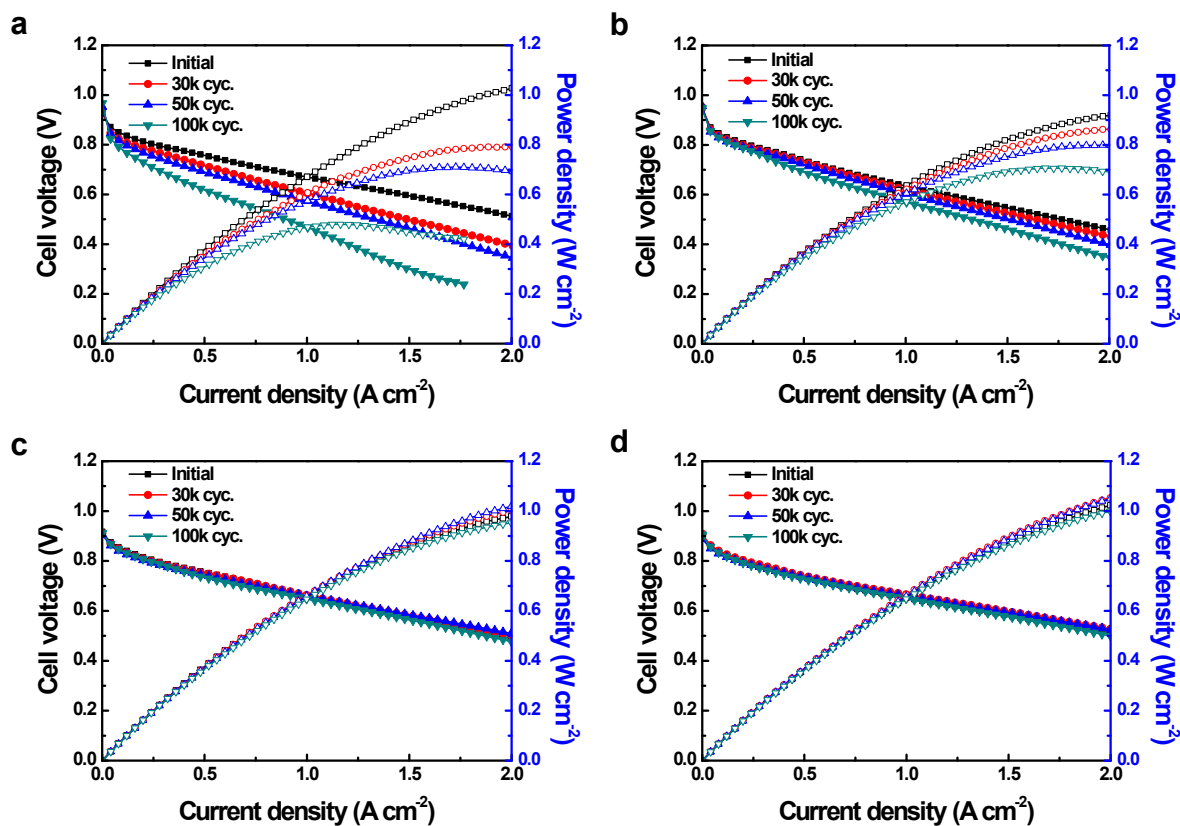


Figure S10 Polarization curves of (a) Pt/C, (b) Pt@CS/CNF600, (c) Pt@CS/CNF700 and (d) Pt@CS/CNF900. Solid and open symbols represent the cell voltage and power density, respectively. The loading amounts of Pt were $0.1 \text{ mg}_{\text{Pt}} \text{ cm}^{-2}$ and $0.125 \text{ mg}_{\text{Pt}} \text{ cm}^{-2}$ for the anode and cathode, respectively. During the cell evaluation, 150 sccm of H_2 and 300 sccm of O_2 were fed to the anode and cathode, respectively. The AST cycling was performed at 70°C with H_2 (100 sccm) and N_2 (30 sccm) gases fed to the anode and cathode, respectively. In the AST cycling, the potential was cycled repetitively by potential steps between 0.6 V (3 s) and 0.95 V (3 s) with rise time of 0.1 s. All reactant gases were fully humidified before fed.

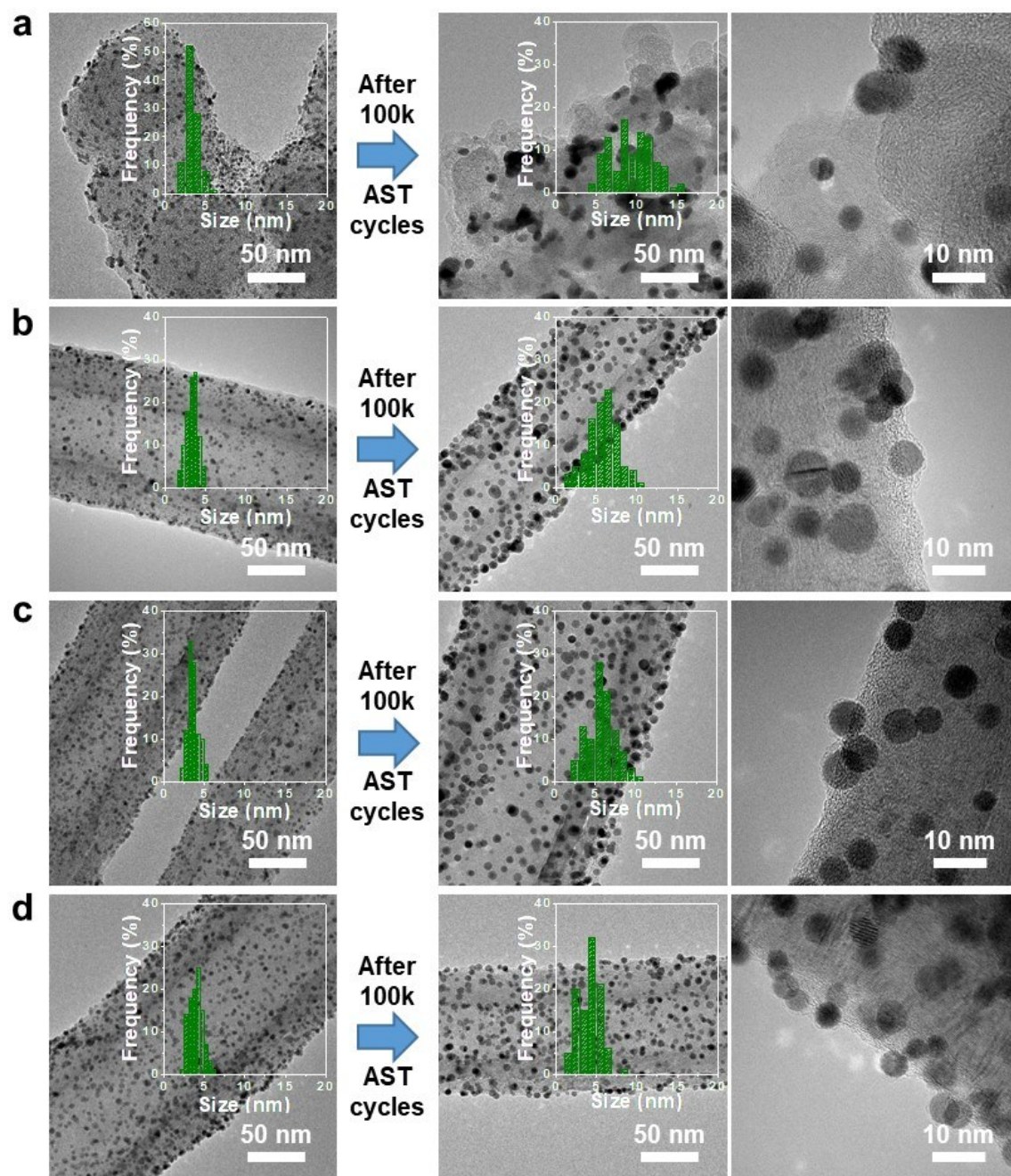


Figure S11 TEM images of (a) Pt/C, (b) CS@Pt/CNF600, (c) CS@Pt/CNF700 and (d) CS@Pt/CNF900 before and after 100k AST cycles in a unit cell.